Journal of Assisted Reproduction and Genetics (2021) 38:2791–2799
https://doi.org/10.1007/s10815-021-02295-x

GENETICS

Pathogenesis of acephalic spermatozoa syndrome caused by splicing mutation and de novo deletion in *TSGA10*

Mingfei Xiang[1,2,3,4] · Yu Wang[1,2,3,4] · Weilong Xu[5] · Na Zheng[1,2,3,4] · Jingjing Zhang[1,2,3,4] · Zongliu Duan[1,2,3,4] · Xiaomin Zha[1,2,3,4] · Xuanming Shi[6] · Fengsong Wang[5] · Yunxia Cao[1,2,3,4] · Fuxi Zhu[1,2,3,4]

Received: 10 June 2021 / Accepted: 3 August 2021 / Published online: 18 August 2021

Abstract

Purpose To identify the genetic causes for acephalic spermatozoa syndrome.

Methods Whole-exome sequencing was performed on the proband from a non-consanguineous to identify pathogenic mutations for acephalic spermatozoa syndrome. Quantitative real-time polymerase chain reaction and whole genome sequencing were subjected to detect deletion. The functional effect of the identified splicing mutation was investigated by minigene assay. Western blot and immunofluorescence were performed to detect the expression level and localization of mutant TSGA10 protein.

Results Here, we identified a novel heterozygous splicing mutation in *TSGA10* (NM_025244: c.1108-1G > T), while we confirmed that there was a de novo large deletion in the proband. The splicing mutation led to the skipping of the exon15 of *TSGA10*, which resulted in a truncated protein (p. A370Efs*293). Therefore, we speculated that the splicing mutation might affect transcription and translation without the dosage compensation of a normal allele, which possesses a large deletion including intact *TSGA10*. Western blot and immunofluorescence demonstrated that the very low expression level of truncated TSGA10 protein led the proband to present the acephalic spermatozoa phenotype.

Conclusion Our finding expands the spectrum of pathogenic TSGA10 mutations that are responsible for ASS and male infertility. It is also important to remind us of paying attention to the compound heterozygous deletion in patients from non-consanguineous families, so that we can provide more precise genetic counseling for patients.

Keywords Male infertility · Teratozoospermia · Acephalic spermatozoa syndrome · *TSGA10* · Spermatogenesis

Introduction

Although not a life-threatening condition, with increasing incidence of reproductive disorders, infertility will be the third major disease threatening human health in the twenty-first century

Mingfei Xiang, Yu Wang and Weilong Xu contributed equally to this work.

✉ Fengsong Wang
fengsongw@ahmu.edu.cn

✉ Yunxia Cao
caoyunxia6@126.com

✉ Fuxi Zhu
fxzhu@ahmu.edu.cn

[1] Reproductive Medicine Center, Department of Obstetrics and Gynecology, the First Affiliated Hospital of Anhui Medical University, Hefei 230022, Anhui, China

[2] NHC Key Laboratory of Study On Abnormal Gametes and Reproductive Tract (Anhui Medical University), Hefei 230032, Anhui, China

[3] Key Laboratory of Population Health Across Life Cycle (Anhui Medical University), Ministry of Education of the People's Republic of China, Hefei 230032, Anhui, China

[4] Anhui Province Key Laboratory of Reproductive Health and Genetics, Anhui Medical University, Hefei 230022, Anhui, China

[5] School of Life Science, Anhui Medical University, Hefei 230022, Anhui, China

[6] Department of Biochemistry and Molecular Biology, Anhui Medical University, Hefei 230032, Anhui, China

according to the WHO [1]. About 50% of infertility can be ascribed to males [2]. Acephalic spermatozoa syndrome (ASS) is a severe condition associated with male infertility. The typical ASS patients' sperm consisted of a large number of headless sperm tails, a few tailless sperm heads, and sperm with abnormal head–tail connection [3]. Since ASS was first discovered in 1977, only a small number of genetic factors, such as *SUN5* [4–10], *PMFBP1* [9, 11–13], *BRDT* [14], *HOOK1* [15], *DNAH6* [16], *TSGA10* [9, 17, 18], and *CEP112* [19] mutations, have been proven to be associated with it, and there were still many cases that could not be explained by the reported genes and mutations, which remained to be elucidated.

TSGA10 (testis specific, 10) is expressed exclusively in testis [20]. It encoded a protein of 82 KDa, including a 27-KDa N-terminus localized in the principal piece, and a 55-KDa C-terminus accumulated in the midpiece of sperm to the centrosome and basal body [21]. Previous studies revealed that TSGA10 played an important role in the assembly of centriole in the head–tail connection, the arrangement of mitochondrial sheath, and the development of embryo [17, 18, 22, 23]. However, there were only several studies about *TSGA10* reported since 2017, the first time linked it with ASS [9, 17, 18].

In the present study, we identified a novel splicing mutation (NM_025244: c.1108-1G > T) in *TSGA10* and a de novo large deletion contained intact *TSGA10*. This is the first case reported as a heterozygous deletion in *TSGA10*. Our finding expanded the spectrum of pathogenic *TSGA10* mutations responsible for ASS and male infertility.

Materials and methods

Human subjects

The proband was recruited from Reproductive Medicine Center, Department of Obstetrics and Gynecology, the First Affiliated Hospital of Anhui Medical University. The proband's sperm met with a certain diagnostic standard of ASS according to the World Health Organization 2010 guidelines [1]. We obtained informed consent from all the participants, and the study was approved by the Ethics Committee of Anhui Medical University.

Papanicolaou staining

Papanicolaou staining was performed according to the World Health Organization standards for human semen examination and processing [1] to assess sperm morphology.

WES and co-segregation analysis

Genomic DNA was extracted following the protocol of the QIAamp DNA blood midi kit (Qiagen, Hilden, Germany). We performed WES on the proband and filtered out the most promising candidate mutations using the methods described in our previous studies [4, 11], except that we took the compound heterozygous mutations into consideration due to the proband from a non-consanguineous family.

The suspected mutation in *TSGA10* was subjected to co-segregation analysis by Sanger sequencing using the primers shown in Table 1. As the discrepancy of the law of co-segregation, we speculated on the existence of the compound heterozygous deletion.

qPCR and WGS

To verify our speculation, the expression level of *TSGA10* in proband and his parents were analyzed by qPCR. Primers for qPCR are shown in Table 1. qPCR was performed using TB Green Premix Ex Taq II (Tli RNase H Plus) (Takara Biomedical Technology, Beijing, China) in StepOnePlus™ Real-Time PCR System with Tower (Applied Biosystems, Foster City, CA). Forty cycles of denaturation at 95℃ for 5 s, annealing at 60℃ for 30 s were performed. Results were analyzed by the $2^{-\Delta\Delta CT}$ method. The expression of GAPDH served as reference gene and the proband's father, as a heterozygote, served as the normal control. Each reaction was repeated three times.

WGS was performed on the proband to find the definite deletion range and fracture site further. Briefly, eligible DNA was broken into fractions followed with repaired and amplified. Then, the library was constructed by ligating the fractions. Finally, high qualitative reads were compared with the human genome and the unique reads were extracted and analyzed. Polymerase chain reaction (PCR) and Sanger sequencing were followed to confirm the breakpoint and the primers are also shown in Table 1.

Minigene assay

The c.1108-1G > T mutation was located at the acceptor splice site of intron 14. Due to the large size of intron, we were unable to clone the full sequence from exon 14 to exon 16 into the minigene vector. Thus, we integrated exon14, exon 15, exon 16, and the sequences 150–200 bp before and after every exon by PCR and cloned the integrated fragment into a pcDNA3.1 plasmid using the method of homologous recombination. The mutation was generated by Mut Express® II Fast Mutagenesis Kit V2 (Vazyme Biotech, Nanjing, China). The wild type and mutant plasmids were transfected into HEK293T cells, respectively. After incubation for 36 h, total RNA was extracted using trizol and subjected to reverse transcription-polymerase chain reaction (RT-PCR) with HyperScriptTM III RT SuperMix for qPCR with gDNA Remover (NovaBio, Shanghai, China) following the manufacturer's

Table 1 *TSGA10* primers used for PCR

Target	Forward	Reverse
Primers used for co-segregation analysis		
exon15: c.1108-1G > T	TGCTTATTTGGGTCATTTGCC	ACCTGTCGTTCTGAGTATACCA
Primers used for real-time PCR		
Exon6	AAGTCCAAGACGCCCATCAC	ACTGTGCCATCAAAGAGACCTC
Exon7	TGGCAGAAATTCAGGGTAATG	TTGCAGGTTTAAGCAGTCTCAT
Exon8	ATTACCCGACTTCGACG	CTTTCCAACCTTTAGCCTC
Exon9	AGAAGGCTCACCTGGAA	CCATTGAGTGTTTATAGCCA
Exon10	TCCTGTCAGTCTTGCCAT	CTTTTTGTCTGCCAAGTTC
Exon11	CTTTCTGATACTCAGCGACACC	GTTAAGGGCTTGTTTCCAAGTT
Exon12	GGAGAAGTTCAAAAAGTACGATA	GCCAGATCATTGAGGGTTC
Exon13	ATCATTGCTGAGATGGAACA	CGTATCATTAAGCCCCTTG
Exon14	CTTGTGAGAATTTGTTGCTCTG	CTTTCCCTGGCGATCTGG
Exon15	TGGAGGTTAACAAGCTGAAGAA	CTTTGATTCACCTGTCGTTCTG
Exon16	CAGGAATCTGAGAACCG	CAGCAGTGATAAGTTCCAG
Exon17	AGGTCTTACAAGTCCCAG	CAAGTTTAATACAGAGTTCCC
Exon18	TGAACTCCTGAGGAGTCAGATG	TTTTCTGCCAAACAAAGGTG
Exon19	GAGTAGAGATGTGGCCCAG	AGAACTAAAACCTCTTGTTACCTA
Exon20	GCCGTACAAGAACTTCGC	GATGGTGAGCACGTTCTG
Exon21	CTTACGTTTTGCTGAAGTGATACAC	TTGACCTTTCTCAGGGATGTG
Primers used to confirm the breakpoint		
Breakpoint	ACTCAGGTGATGATTTTATGGG	ACCCTCTAACTTGCTCTGCCC
Primers used for constructing the minigene vectors		
Exon14	CTATAGGGAGACCCAAGCTTACAGTGT ACTGAGGCCCTAA	GAAAACACATAAGCCCAATAGCATTCC ATTTAAAAATTATGTGGCCTA
Exon15	TAGGCCACATAATTTTTAAATGGAATG CTATTGGGCTTATGTGTTTTC	GAAAACAGGTCATCCTGTAATTAACAT CCAGGCATCTTTCTGAACA
Exon16	TGTTCAGAAAGATGCCTGGATGTTAAT TACAGGATGACCTGTTTTC	ACGTCATATGGATAGGATCCTTGCTCA ACCTCTCTGTTG
Primers used for site directed mutagenesis		
Mu1108-1	TTTTTTCGTATGCACTGTCCAAAAAAT TGAATGACACTC	TGGACAGTGCATACGAAAAAAAGATAG GTATATTTGACTATG
Primers used for detecting splicing isoform		
Exon14-16	ACAGTGTACTGAGGCCCTAA	TTGCTCAACCTCTCTGTTG

instructions. PCR was performed to amplify and compare the *TSGA10* transcript from the wild type and mutant plasmids. The primers for constructing the minigene vectors and for detecting alternative splice sites are listed in Table 1.

Western blot and immunofluorescence

Western blot and immunofluorescence were performed to detect the expression level and localization of mutant TSGA10 protein compared with the normal, in accordance with the methods described previously [4, 11, 13]. The detailed information of antibodies we used displayed in Table 2.

Results

Clinical findings

We recruited an ASS patient from a non-consanguineous family (Fig. 1a). The proband did not have any bad living habits or any adverse chemical contact history. Examination of the patient revealed normal development of male external genitalia, normal bilateral testicular size, and no abnormality upon palpation. The chromosomal karyotype of the patient was normal 46, XY. The hormonal levels of the proband were normal. The characteristics of the patient's semen are shown in Table 3. Notably, it exhibited that spermatozoa of proband with normal morphology

Table 2 Antibodies used in Western blot and immunofluorescence

Primary/secondary antibodies	Host species	Company	Cat/Lot no	Application	Dilution
TSGA10 Antibody	Rabbit	Proteintech	12,593–1-AP	WB	1:2000
				IF	1:200
Acetyl-α-Tubulin Rabbit mAb	Rabbit	ABclonal	5335 T	WB	1:2000
				IF	1:1000
Alexa Fluor® 488—Conjugated Goat anti-Mouse IgG(H + L)	Goat	ThermoFisher	1,834,802	IF	1:400
Alexa Fluor® 555—Conjugated Goat anti-Rabbit IgG(H + L)	Goat	ThermoFisher	1,774,719	IF	1:400
Goat anti-Rabbit IgG (H + L) Secondary Antibody, HRP	Goat	ThermoFisher	31,460	WB	1:5000
Goat anti-Mouse IgG (H + L) Secondary Antibody, HRP	Goat	Thermofisher	31,430	WB	1:5000

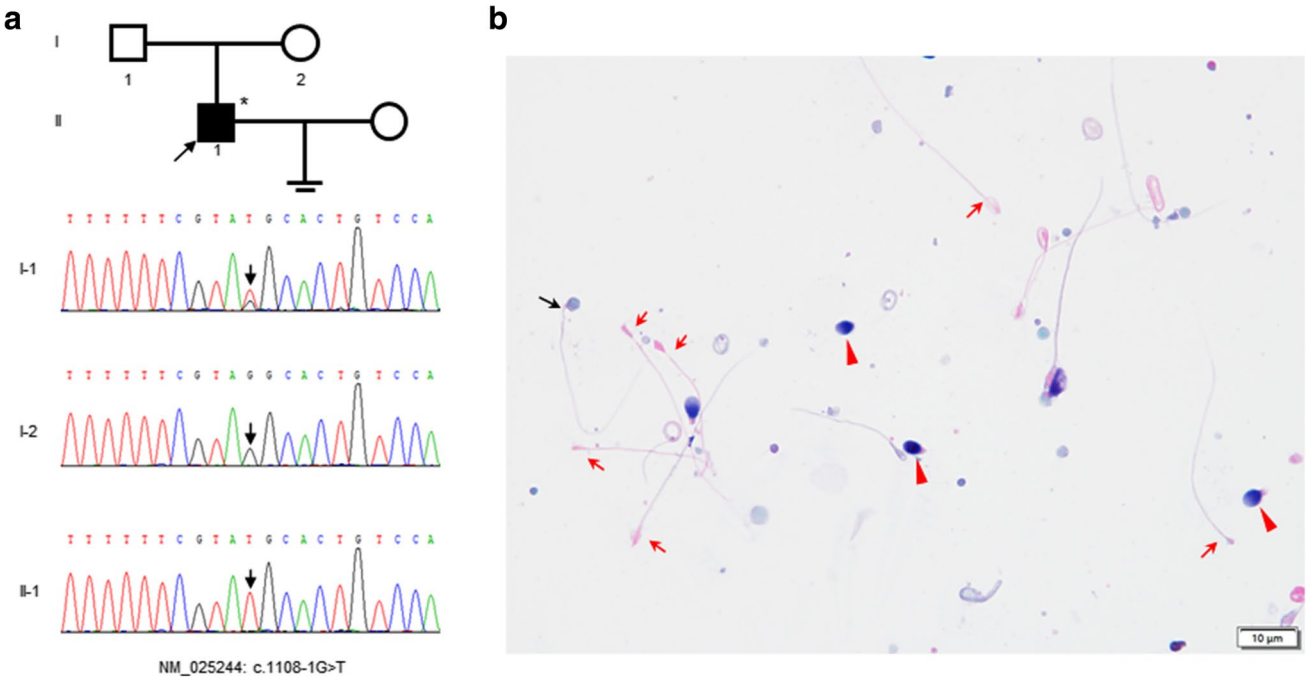

Fig. 1 The family pedigree of the proband and papanicolaou staining of his sperm. **a** The family tree shows a patient with acephalic spermatozoa syndrome in a non-consanguineous pedigree. The black square shows the affected individuals with *TSGA10* mutation and an arrow indicates the proband. The arrows in the chromatograms show the position of the mutation. The asterisk stands for the proband subjected WES. **b** Papanicolaou staining of the proband's sperm. The sperm morphology was primarily acephalic (red arrow). Besides, there also were a few tailless heads (red arrowhead) and a small proportion of intact spermatozoa with abnormal head–tail junction (black arrow) can be observed. Scale bars: 10 μm

Table 3 Statistical analysis of the semen parameters

Proband	First ejaculate	Second ejaculate	Reference value
Volume (ml)	2.6	2.7	≥ 2
Concentration ($\times 10^6$/ml)	0.6	1.3	≥ 20
Motility a + b (%)	0	0	≥ 50
Percentages of different morphologic spermatozoa(%)			
Normally formed	1	1	≥ 23%
Abnormal head–tail junction	0.2	0.1	/
Decaudated	0.7	1	/
Acephalic	98.1	98.9	/

Table 4 Screening strategy to identify the causal genes by WES

Screening procedure	The proband (II-1)
Total variants	153,484
Filter rare variants (not reported or frequency < 0.1%) in public databases[a]	2491
Coding (nonsynonymous exonic, indel or splice site variant)	363
Predicted to be highly deleterious	41
Relevancy for phenotype[b]	1

[a] represent the following three databases: 1000 Genomes variant database, Genome Aggregation Database, and Exome Aggregation Consortium; [b] represents mutations associated with phenotype, including expression in testis or not reported

comprised 1% of the population, while ~ 98% were headless tails through Papanicolaou staining (Fig. 1b).

Genetic analysis

According to previous work suggested a genetic origin, WES was performed on the proband to identify the genetic defect. After screening with all our criteria, 41 mutations were noted (Table 4). The splicing mutation in *TSGA10* is viewed as the most possible pathogenesis of the proband on the basis of previous studies. However, our results of Sanger sequencing demonstrated that the proband (II-1) was homozygous for the splicing mutation; his father (I-1) was heterozygous, while his mother (I-2) was a wild type, which

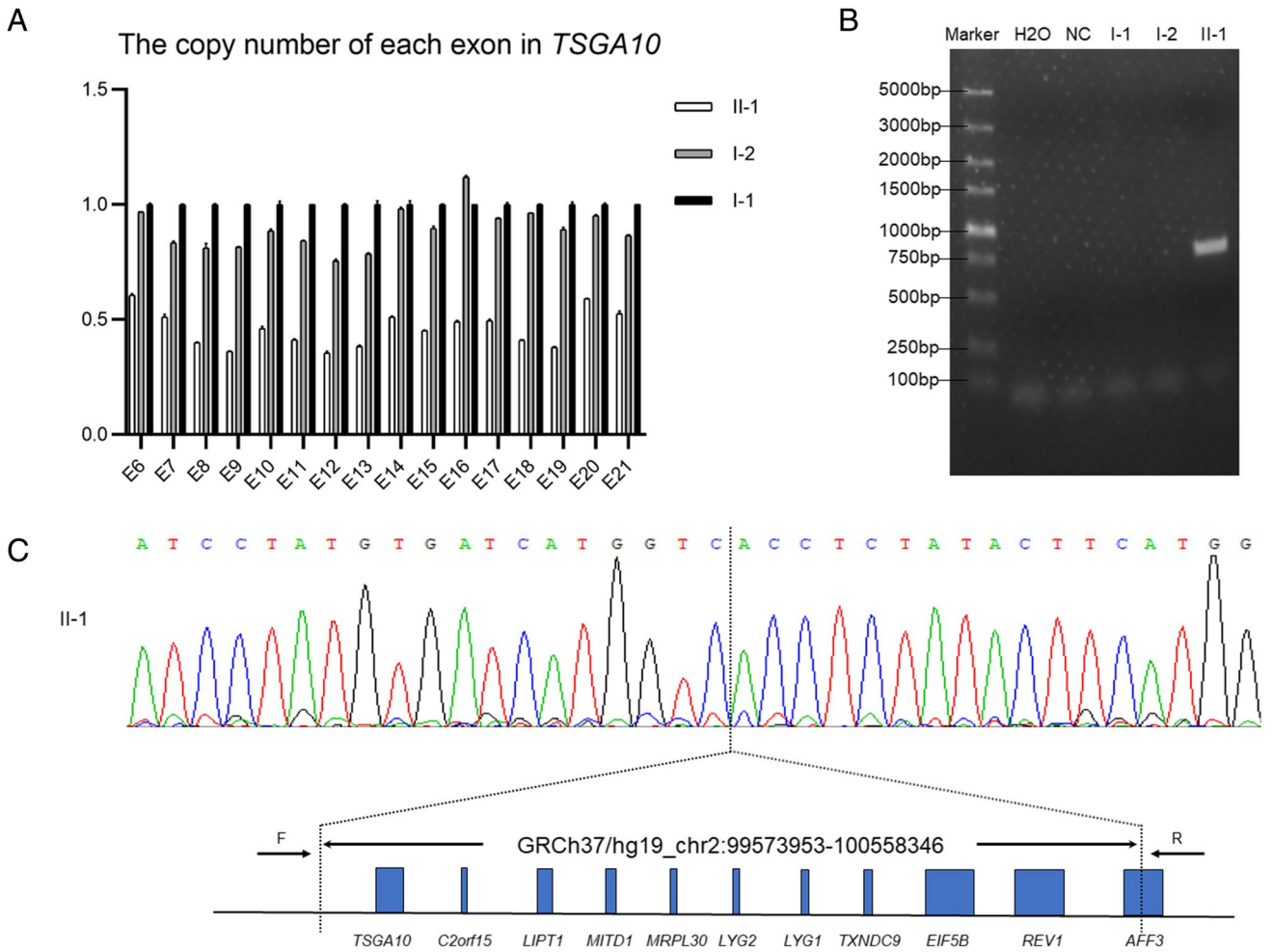

Fig. 2 Identification of the large deletion. **a** Detected heterozygous deletions in exons of *TSGA10* in the proband and his parents with qPCR. **b** The DNA fragment containing the breakpoint was amplified with PCR using the special primers, shown in the Table 1, designed based on the WGS. **c** The sequencing result of the DNA fragment above shows an 984,394 bp deletion spanning the eleven genes, contained the entire *TSGA10* gene

Table 5 CNVs detected by WGS

Chr	Start	End	Length	Type	Ratio	Cutoff	Gene
2	99572631	100558590	985959	Del*1	0.45	> 100 kb	REV1 (NM_001037872, NM_016316); AFF3 (NM_001025108, NM_002285); TSGA10 (NM_182911, NM_025244); C2orf15 (NM_144706); LIPT1 (NM_015929, NM_145197, NM_145198, NM_145199, NM_001204830); MITD1 (NM_138798); MRPL30 (NM_145212); LYG2 (NM_175735); LYG1 (NM_174898); TXNDC9 (NM_005783); EIF5B (NM_015904)
4	70121496	70235854	114358	Del*1	0.63	> 100 kb	UGT2B28(NM_001207004, NM_053039)
8	39,229,215	39387492	158277	Del*1	0.43	> 100 kb	NULL
6	11392006	11454521	62515	Dup*3	1.37	/	NULL
7	102110025	102207359	97334	Dup*3	1.86	/	LRWD1(NM_152892); POLR2J(NM_006234); POLR2J3(NM_001097615); SPDYE2(NM_001031618); SPDYE2L(NM_001166339)
9	210770	269060	58290	Dup*3	1.17	/	C9orf66 (NM_152569); DOCK8(NM_203447);
17	34485533	34579126	93593	Del*1	0.84	/	TBC1D3B(NM_001001417); CCL3L3(NM_001001437); CCL3L1(NM_021006); CCL4L1(NM_001001435); CCL4L2(NM_207007)
19	53931213	54006794	75581	Dup*3	1.42	/	ZNF761(NM_001008401); ZNF813(NM_001004301)

Del*1 represents one copy and Dup*3 represents three copies

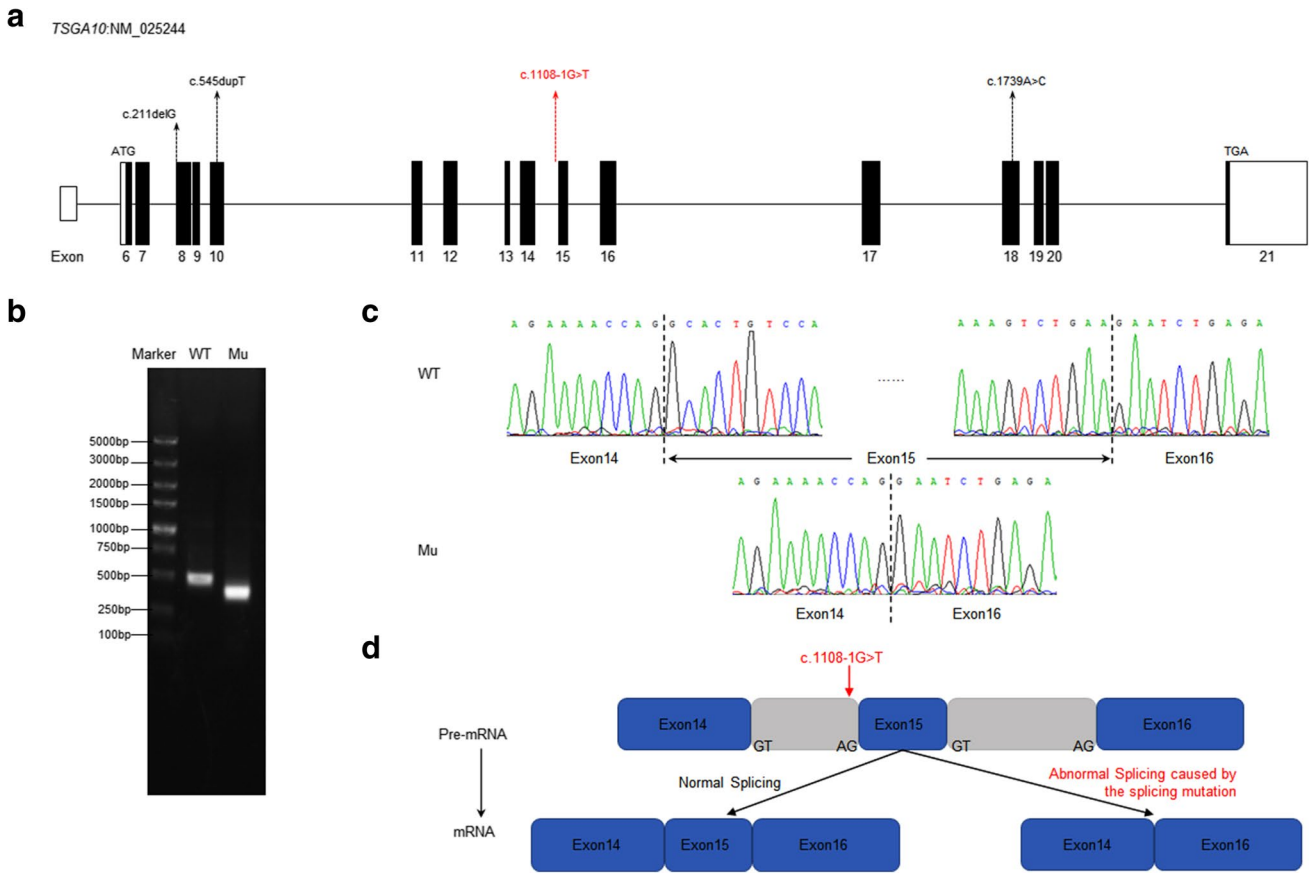

Fig. 3 The location and conservation of the mutant residue in *TSGA10*. **a** The location of mutations in the *TSGA10* exons. Mutations described in the previous study are marked in black and the novel splicing mutation identified in our study is marked in red. **b** Agarose gel electrophoresis illustrating the effect of the TSGA10 c.1108-1G>T mutation. Compared with the wild type lane, the mutation lane showed a smaller band. **c** Identified the abnormal splicing isoform of the mutation. By RT-PCR and Sanger sequencing, the results showed that the splice-site mutation in *TSGA10* lead to the skipping of exon15. **d** A possible scheme illustrating of the effect of the *TSGA10* c.1108-1G>T mutation. In this case, the mutation skips the canonical receptor site leading to the entire deletion of exon15 in cDNA and resulting in abnormal transcription and translation

were not in conformity with co-segregation (Fig. 1a). Therefore, we speculated that there was the possibility of deletion in *TSGA10*.

Identification of the large deletion

To confirm whether the deletion exists, we performed qPCR analysis on DNA from the proband and his parents to detect possible heterozygous deletions in *TSGA10*. Heterozygous deletion encompassing all of the exons of *TSGA10* was identified in the proband compared with his parents, suggesting the deletion of the whole *TSGA10* (Fig. 2a). To confirm qPCR results and identify the deletion range, WGS was performed on the proband and eight copy number variants (CNV) were identified (Table 5). Among them, a large heterozygous deletion, involved eleven genes, contained intact *TSGA10*, was detected (Fig. 2c). Moreover, the deletion range was ascertained to uncover 984,394 bp (chr2:99,573,953–100,558,346) and the breakpoint was identified by PCR using the specific primers designed on the basis of the WGS result (Fig. 2b, c).

The influence of the splicing mutation in *TSGA10* in vitro

The splicing mutation in *TSGA10* is located in the canonical receptor site of intron 14 (Fig. 3a, d). In order to study the effect of the splicing mutation NM_025244 (*TSGA10*) c.1108-1G > T, we performed a minigene assay. As agarose gel electrophoresis showed, we got two different sizes of RT-PCR productions from the wild type and the splicing mutation minigenes, respectively (Fig. 3b). The following Sanger sequencing indicated the abnormal splicing isoform of the mutation compared with the wild type (Fig. 3c). We found that the splicing mutation led to the skipping of the exon15 of *TSGA10*, which resulted in a frameshift and a predicted truncated protein (p. A370Efs*293) (Fig. 3d). The losing residue affected by the splicing mutation is conserved among different species (Fig. 4a).

Expression and localization of TSGA10

In order to verify the effect of the mutation and deletion, Western blot and immunofluorescence assays were performed to detect the expression level and localization of mutant TSGA10 protein in the proband's sperm compared with the normal control. Western blot analysis demonstrated that TSGA10 was expressed in the control as its theoretical molecular weight, but was lower and decayed significantly from the proband's sperm (Fig. 4b), which was consistent with the result of minigene assay. By immunostaining the spermatozoa from a normal control, TSGA10 was found to localize at the head–tail junction of spermatozoa (Fig. 4c). However, no staining was observed in the proband's sperm (Fig. 4c).

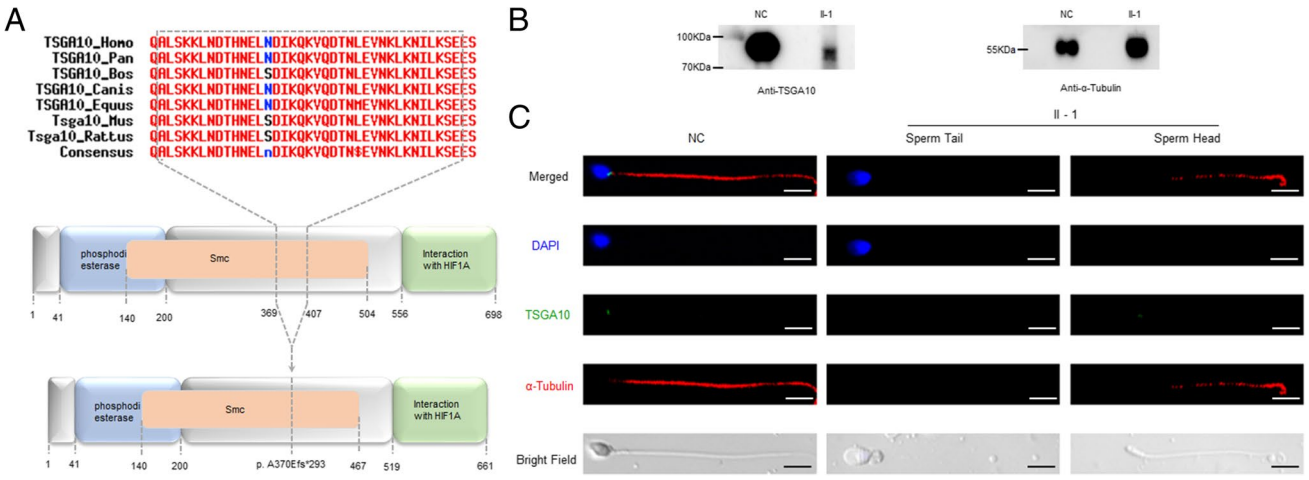

Fig. 4 Expression and localization of TSGA10 in the proband's sperm compared with the normal. **a** Domains in the TSGA10, the predicted mutant TSGA10. The full-length protein is 698 amino acids (aa). Domain with putative phosphodiesterase activity, aa 41 to 200 (blue box); domain that can interact with HIF1A, aa 556 to 689 (green box); the maintenance of the chromosome (Smc) domain, aa 140 to 504 (orange box). The p. A370Efs*293 mutation is located at the Smc domain of the TSGA10 protein and the truncated protein harbors a 293aa frameshift sequence. The 37aa, which was truncated, presented high-conserved among different species. **b** Western blot was performed on the proband's sperm, using the normal sperm as a control. **c** The immunostaining of the proband's sperm compared with the normal. The nucleus and tail of the sperm are stained with DAPI (blue) and α-Tubulin (red), respectively. The localization of TSGA10 in sperm from the proband and normal control were demonstrated by immunofluorescence staining with TSGA10 antibody (green). Scale bars: 5 μm

Discussion

TSGA10 is a testis-specific protein, which is located to the principal piece of sperm, to the centrosome and basal body [20, 21]. Previous studies revealed that TSGA10 played an important role in the assembly of centriole in the head–tail connection, the arrangement of mitochondrial sheath, and the development of embryo [17, 18, 22, 23]. So far, TSGA10 mutations, as the definitive genetic etiology, have been associated with about 3.1% cases which had reported [4–19].

Here, we identified a novel splicing mutation (c.1108-1G > T) in *TSGA10* in an ASS patient from a non-consanguineous family (Fig. 1a). At the same time, we found a large deletion in the proband involved eleven genes, contained intact *TSGA10*, by qPCR and WGS due to the violation of co-segregation principle (Fig. 2). The other ten genes, except for *TSGA10*, were never reported to be associated with male infertility so far. Besides, we made a sketchy exploration of this large deletion. On the basis of the sequences of the deletion, we found that it existed line interspersed nuclear elements on the bilateral sides of the deletion, which may cause non-sister chromatids mismatch and unequal exchange to result in the deletion. However, the detailed pathogenic mechanism needs to be explained further.

By the minigene assay, we found that the splicing mutation led to the skipping of the exon15 of *TSGA10* (Fig. 3c, d), and a truncated protein (p. A370Efs*293), which impaired the function of structural maintenance of the chromosome (Smc) domain of TSGA10 (Fig. 4a). Consistent with the minigene assay, Western blot showed a truncated TSGA10 protein (about 78KDa) in the proband, which was lower than its theoretical molecular weight and decayed significantly (Fig. 4b). Immunostaining was not observed in the proband's sperm, compared with the normal, which staining was located in the head–tail junction of sperm (Fig. 4c). According to the result of Western bolt, the signal might not be detected, causing by its appreciable decay. Therefore, we considered that the ASS of the proband caused by the novel splicing mutation and deletion in TSGA10.

We herein summarized known data on the gene *TSGA10* contribution of genes to acephalic spermatozoa (Fig. 3a) and broadened the spectrum of genetic causes. Furthermore, the identification of heterozygous deletion suggested that pathogenic genes we known might contribute more than we found in patients with ASS because genomic deletions cannot be screened by WES. All our studies were devoted to potentially facilitating diagnoses and promoting therapeutic development.

Acknowledgements We would like to sincerely thank the patient and his family for participation.

Author contribution F.Z., Y.C., and F.W. conceived and designed the experiments. J.Z., Z.D., and X.Z. collected the samples. M.X., Y.W., W.X., and N.Z. performed the experiments. F.Z., Y.C., F.W., M.X., Y.W., and X.S. analyzed the data. Y.W. and M.X. wrote the article. All authors approved the final article.

Funding National Natural Science Foundation of China (82071701 to F. Z.; 81792641 to F. W.), Natural Science Foundation of Anhui Province (1908085J28 to F. Z.), Key R&D program of Anhui Province (201904a07020050 to F. Z.), the Non-profit Central Research Institute Fund of Chinese Academy of Medical Sciences (2019PT310002), and Scientific Research Foundation of the Institute for Translational Medicine of Anhui Province (SRFITMAP 2017zhyx29 and ZHYX2020A001) supported this study.

Data availability The data underlying this article are available in the article.

Code availability Not applicable

Declarations

Ethics approval This study was approved by the Ethics Committee of Anhui Medical University. Written informed consent was obtained from each participant.

Consent to participate Obtained.

Consent for publication Obtained.

Conflict of interest The authors declare no competing interests.

References

1. World Health Organization. WHO Laboratory Manual for the Examination and Processing of Human Semen, 5th edn. Cambridge: Cambridge University Press, 2010;37–44:65–67.
2. Mascarenhas MN, Flaxman SR, Boerma T, Vanderpoel S, Stevens GA. National, regional, and global trends in infertility prevalence since 1990: a systematic analysis of 277 health surveys. PLoS Med. 2012;9(12):e1001356. https://doi.org/10.1371/journal.pmed.1001356.
3. Chemes HE, Carizza C, Scarinci F, Brugo S, Neuspiller N, Schwarsztein L. Lack of a head in human spermatozoa from sterile patients: a syndrome associated with impaired fertilization. Fertil Steril. 1987;47(2):310–6. https://doi.org/10.1016/s0015-0282(16)50011-9.
4. Zhu F, Wang F, Yang X, Zhang J, Wu H, Zhang Z, et al. Biallelic SUN5 mutations cause autosomal-recessive acephalic spermatozoa syndrome. Am J Hum Genet. 2016;99(4):942–9. https://doi.org/10.1016/j.ajhg.2016.08.004.
5. Elkhatib RA, Paci M, Longepied G, Saias-Magnan J, Courbiere B, Guichaoua MR, et al. Homozygous deletion of SUN5 in three men with decapitated spermatozoa. Hum Mol Genet. 2017;26(16):3167–71. https://doi.org/10.1093/hmg/ddx200.
6. Sha YW, Xu X, Ji ZY, Lin SB, Wang X, Qiu PP, et al. Genetic contribution of SUN5 mutations to acephalic spermatozoa in Fujian China. Gene. 2018;647:221–5. https://doi.org/10.1016/j.gene.2018.01.035.

7. Fang J, Zhang J, Zhu F, Yang X, Cui Y, Liu J. Patients with acephalic spermatozoa syndrome linked to SUN5 mutations have a favorable pregnancy outcome from ICSI. Hum Reprod. 2018;33(3):372–7. https://doi.org/10.1093/humrep/dex382.
8. Shang Y, Yan J, Tang W, Liu C, Xiao S, Guo Y, et al. Mechanistic insights into acephalic spermatozoa syndrome-associated mutations in the human SUN5 gene. J Biol Chem. 2018;293(7):2395–407. https://doi.org/10.1074/jbc.RA117.000861.
9. Liu G, Wang N, Zhang H, Yin S, Dai H, Lin G, et al. Novel mutations in PMFBP1, TSGA10 and SUN5: Expanding the spectrum of mutations that may cause acephalic spermatozoa. Clin Genet. 2020;97(6):938–9. https://doi.org/10.1111/cge.13747.
10. Zhang D, Huang WJ, Chen GY, Dong LH, Tang Y, Zhang H, et al. Pathogenesis of acephalic spermatozoa syndrome caused by SUN5 variant. Mol Hum Reprod. 2021;27(5):gaab028. https://doi.org/10.1093/molehr/gaab028.
11. Zhu F, Liu C, Wang F, Yang X, Zhang J, Wu H, et al. Mutations in PMFBP1 cause acephalic spermatozoa syndrome. Am J Hum Genet. 2018;103(2):188–99. https://doi.org/10.1016/j.ajhg.2018.06.010.
12. Sha YW, Wang X, Xu X, Ding L, Liu WS, Li P, et al. Biallelic mutations in PMFBP1 cause acephalic spermatozoa. Clin Genet. 2019;95(2):277–86. https://doi.org/10.1111/cge.13461.
13. Lu M, Kong S, Xiang M, Wang Y, Zhang J, Duan Z, et al. A novel homozygous missense mutation of PMFBP1 causes acephalic spermatozoa syndrome. J Assist Reprod Genet. 2021;38(4):949–55. https://doi.org/10.1007/s10815-021-02075-7.
14. Li L, Sha Y, Wang X, Li P, Wang J, Kee K, et al. Whole-exome sequencing identified a homozygous BRDT mutation in a patient with acephalic spermatozoa. Oncotarget. 2017;8(12):19914–22. https://doi.org/10.18632/oncotarget.15251.
15. Chen H, Zhu Y, Zhu Z, Zhi E, Lu K, Wang X, et al. Detection of heterozygous mutation in hook microtubule-tethering protein 1 in three patients with decapitated and decaudated spermatozoa syndrome. J Med Genet. 2018;55(3):150–7. https://doi.org/10.1136/jmedgenet-2016-104404.
16. Li L, Sha YW, Xu X, Mei LB, Qiu PP, Ji ZY, et al. DNAH6 is a novel candidate gene associated with sperm head anomaly. Andrologia. 2018. https://doi.org/10.1111/and.12953.
17. Sha YW, Sha YK, Ji ZY, Mei LB, Ding L, Zhang Q, et al. TSGA10 is a novel candidate gene associated with acephalic spermatozoa. Clin Genet. 2018;93(4):776–83. https://doi.org/10.1111/cge.13140.
18. Ye Y, Wei X, Sha Y, Li N, Yan X, Cheng L, et al. Loss-of-function mutation in TSGA10 causes acephalic spermatozoa phenotype in human. Mol Genet Genomic Med. 2020;8(7):e1284. https://doi.org/10.1002/mgg3.1284.
19. Sha Y, Wang X, Yuan J, Zhu X, Su Z, Zhang X, et al. Loss-of-function mutations in centrosomal protein 112 is associated with human acephalic spermatozoa phenotype. Clin Genet. 2020;97(2):321–8. https://doi.org/10.1111/cge.13662.
20. Modarressi MH, Cameron J, Taylor KE, Wolfe J. Identification and characterisation of a novel gene, TSGA10, expressed in testis. Gene. 2001;262(1–2):249–55. https://doi.org/10.1016/s0378-1119(00)00519-9.
21. Modarressi MH, Behnam B, Cheng M, Taylor KE, Wolfe J, van der Hoorn FA. Tsga10 encodes a 65-kilodalton protein that is processed to the 27-kilodalton fibrous sheath protein. Biol Reprod. 2004;70(3):608–15. https://doi.org/10.1095/biolreprod.103.021170.
22. Luo G, Hou M, Wang B, Liu Z, Liu W, Han T, et al. Tsga10 is essential for arrangement of mitochondrial sheath and male fertility in mice. Andrology. 2021;9(1):368–75. https://doi.org/10.1111/andr.12889.
23. Behnam B, Modarressi MH, Conti V, Taylor KE, Puliti A, Wolfe J. Expression of Tsga10 sperm tail protein in embryogenesis and neural development: from cilium to cell division. Biochem Biophys Res Commun. 2006;344(4):1102–10. https://doi.org/10.1016/j.bbrc.2006.03.240.